Materials Science and Engineering C 33 (2013) 1432–1437

Contents lists available at SciVerse ScienceDirect

Materials Science and Engineering C

journal homepage: www.elsevier.com/locate/msec

An experimental confirmation of thermal transitions in native and regenerated spider silks

Fernando G. Torres *, Omar P. Troncoso, Carlos Torres, Wilson Cabrejos

Department of Mechanical Engineering, Catholic University of Peru, Av. Universitaria 1801, Lima 32, Lima, Peru

ARTICLE INFO

Article history:
Received 10 April 2012
Received in revised form 12 November 2012
Accepted 13 December 2012
Available online 22 December 2012

Keywords:
Spider silk
Thermal transitions
Differential scanning calorimetry

ABSTRACT

Biological structures such as spider silks are formed by proteins. The physical properties of such proteins are determined by environmental conditions such as temperature and humidity. In this paper, we confirm the thermal transitions that take place in spider silks using differential scanning calorimetry and study how the interaction of spider silk proteins with water affects the onset temperatures for these thermal processes. Native fibres and regenerated films of dragline silk and egg sac silk from *Argiope argentata* spiders were used to study thermal transitions of protein based structures. For the first time, differential scanning calorimetry (DSC) tests were carried out with spider silk samples of relatively large mass (10 mg). Previous attempts of DSC tests applied to spider silk samples failed to detect thermal transitions in a conclusive way. The tests reported here, however, show thermal transitions on both natural and regenerated samples that are in agreement with results from dynamic mechanical analysis (DMA) tests reported in the literature. The water content on spider silks seems to lower the temperatures at which such thermal transitions take place. The results also confirm that the amorphous regions of native and regenerated spider silk and silk worm silk give rise to similar thermal transitions.

1. Introduction

Silk is a fibrous protein containing highly repetitive sequences of amino acids that are stored as a liquid and processed as fibres when sheared or spun at secretion [1]. Spiders are dependent on the silk they produce throughout their lifespan. Orb-weaving spiders are able to produce up to seven different types of silks, each of which is spun from a discrete gland [2,3]. The amino acid composition of spider silk is mainly formed by glycine, alanine and serine [1,4] and shows a considerable variability between different types of silk even for the same individual along its lifetime [5].

Tubuliform and acinifom silk are used for the construction of protective egg cases. Spider egg cases have revealed a high serine and low glycine content [6]. Serine and glycine have polar/hydrophilic properties because their hydroxyl group is polar while alanine is hydrophobic.

Dragline silk which is secreted by the major ampullate gland is composed of glycine alanine (GA) and poly(A) entities and short repeats of GPGXn entities [7,8]. It has a high ultimate tensile strength value (1.5 GPa) and it is less extensible than other spider silk fibres except for tubuliform silk [2]. Dragline silk exhibits supercontraction, which is the significant reduction in the length of the fibers when exposed to high relative humidity environments or immersed in water [9–12].

Experimental investigations of the structure of silk at a nanoscale revealed that there are two fundamental structural constituents: a highly organized antiparallel beta sheet nanocrystals and a semiamorphous phase that consists of less orderly protein structures [13]. Hydrogen bonding arrays in β sheet nanocrystals reinforce the polymeric network under mechanical stretch, by forming interlocking regions that transfer the load between chains [14] giving a strong molecular cohesion and thus confer strength to the fibre. These crystalline areas are embedded in a semiamorphous matrix [15]. This semiamorphous region is formed by less orderly beta structures, 3 helices and beta turns [16]. The semiamorphous regions in spider silk are believed to confer elasticity to the fibre [13,14].

As part of the quest to produce synthetic spider silk, several procedures have been studied in order to regenerate spider silk. Among these techniques, the use of ionic liquids as solvents has been reported [17,18]. These salts have melting points below 100 °C [19]. Due to their highly ionic nature, they have negligible vapour pressure which makes ionic liquids an interesting alternative for applications in “green chemistry”.

The solubility of ionic liquids depends on the properties of cations and anions [20]. Dymek et al. [21] claimed that the more the cation and anion are able to participate in hydrogen bonding, the greater the solubility of the silk fibroin. The dissolution of silkworm silk is related with the disruption of hydrogen bonding in its internal structure. WAXS and Raman data [20] have confirmed that ionic liquids disrupt the hydrogen bond in the crystalline domain of cocoon silk which is formed by beta sheet structures.

* Corresponding author. Tel./Fax: +51 1 626 2000.
E-mail address: fgtorres@pucp.edu.pe (F.G. Torres).

0928-4931/$ – see front matter © 2012 Elsevier B.V. All rights reserved.
http://dx.doi.org/10.1016/j.msec.2012.12.047

The excellent mechanical properties of spider silk have been studied extensively [22–27]. Experimental studies of spider silk (dragline silk) using DMA in the tensile mode have reported two local glass transitions. The first transition at around −70 °C is attributed to hydrocarbon interactions while the second transition at around 200 °C is accounted to amide segment interactions [24].

Differential scanning calorimetry is one of the most common techniques used for assessing the thermal transition of polymeric materials. DSC curves show thermal events that can be related to structural changes on polymers such as melting, crystallization and vitrification due to the fact that these changes are accompanied by transitions in the thermodynamic properties of polymers. However, DSC has not been successfully used to study the thermal transitions of spider silks. This is mainly due to the difficulties that arise when trying to find thermal transitions with low mass specimens. Osaki [28] performed DSC tests of spider silks of *Yaginumia sia* and *Argiope amoena*. The endothermic peak that they found at 100 °C disappeared after a second run and was accounted for desorption of water molecules adsorbed on spider fibres. Guess and Viney [29] carried out DSC tests of *Nephila clavipes* silk and found the same endothermic peak at 100 °C with a sample mass of only around 1 mg. Cuniff et al. [30] studied the thermal properties of *N. clavipes* silk by means of DSC, TGA and DMA but did not publish any DSC thermogram. By contrast, thermal transitions of silkworm silk studied by means of DSC tests have been extensively reported in the literature [31–34] as *Bombyx mori* silk is readily available in large quantities.

The aim of this paper is to provide an experimental confirmation of thermal transitions occurring in native and regenerated spider silk. Differential scanning calorimetry was used for this purpose since it probably is the most common technique used for determining glass transitions in the polymer field. To the best of our knowledge, this is the first time that spider silk samples of relatively large mass (10 mg) have been used to carry out DSC tests. The thermograms obtained clearly show thermal transitions that, in the past, had been only registered by means of other characterization techniques such as dynamic mechanical analysis (DMA). The effect of water content on these transitions, as well as the changes in thermal transitions that might arise when spider silk is regenerated has also been considered in this study.

2. Materials and methods

2.1. Spider silk

Silk fibres from *Argiope argentata* (Fabricius, 1775), an American species of the *Araneidae* family, were used in this study. Female adult spiders of 3.5–5 mm in prosoma width were collected in the vicinity of Lima outskirts, Peru. They were housed in 30×20×10 cm cages and were fed larval stage mealworms (*Tenebrio molitor*) three times per week.

Whole egg sacs, including tubuliform and acinifom silks, were used in this study. The egg sacs produced by some of the spiders kept in captivity were collected from the cages. They were opened and spider eggs were removed. Then, the sacs were cleaned in distilled water with continuous stirring and dried in air for 1 day. Finally, the egg sacs were dried stored.

Dragline fibres were retrieved directly from spider ampullate glands at a controlled speed (2 cm/s) by using a forced silking process described elsewhere [35,36]. After the forced silking process, the collected dragline fibres were washed in distilled water with continuous stirring. Then, the fibres were dried at ambient temperature for 1 day and finally, placed in dry storage.

2.2. Silkworm silk

Silkworm (*B. mori*) silk fibres (typical length 20 cm) were obtained by boiling cocoons in three 30 minute changes of a 0.5 % (w/v) Na_2CO_3 aqueous solution in order to extract the glue like sericin protein. The material recovered was then rinsed thoroughly with distilled water. The degummed silk was dried at ambient temperature for 1 day and finally, placed in dry storage.

2.3. Regenerated spider silk films

Both, dragline fibres and egg sacs were dissolved and used to prepare films. The spin dope was prepared from spider silk in ionic liquid 1-butyl-3-methylimidazolium chloride (BMIC). The stored silk fibres were chopped and mixed at 95 °C with BMIC to make a 5% (w/w)

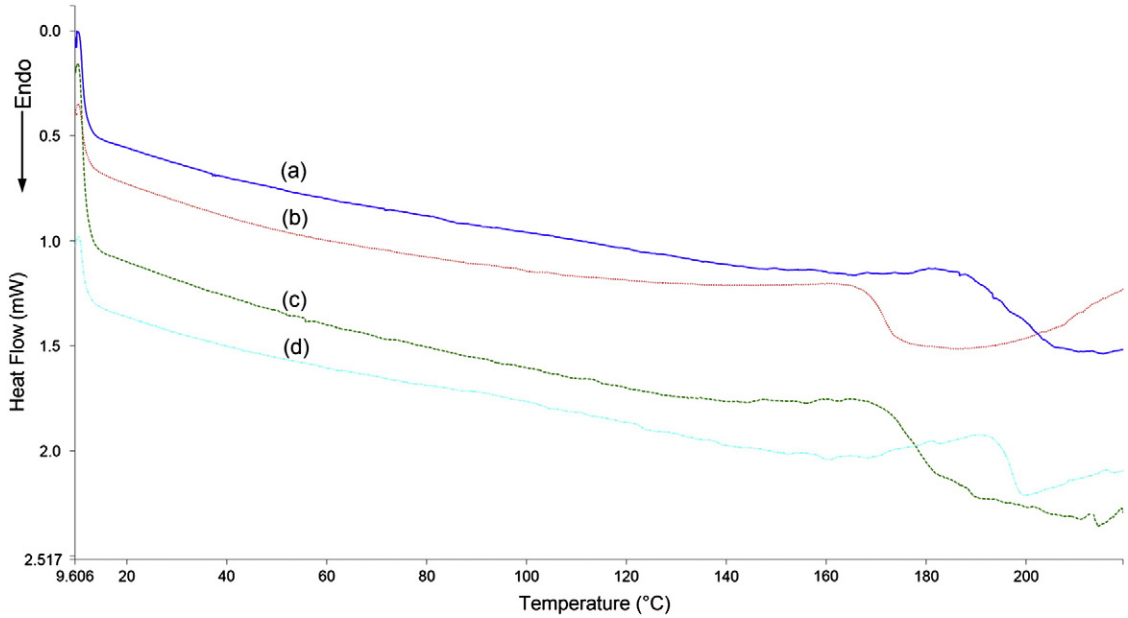

Fig. 1. Representative thermograms of (a) regenerated dragline film, (b) native egg sac silk, (c) regenerated egg sac film and (d) forced dragline silk. Water content of the samples shown is 10% (w/w).

dope solution. After 1.5 h silk fibres were completely dissolved and distilled water was added in order to decrease the dope solution viscosity. The dope was cast on a glass substrate by using a syringe and let cool down for 1 h. The resulting film was then immersed on a methanol bath for 1 h in order to remove the ionic liquid from the film. Finally, the film was dried in air and stored.

2.4. Thermal analysis

Differential scanning calorimetry (DSC) measurements were performed with a Perkin-Elmer DSC-4000 calorimeter. Samples of around 10 mg in mass were heated from 10 °C to 350 °C at a heating rate of 2 °C/min. The samples were prepared and moisturized in a thermogravimetric scale at room temperature. While the pans were still open, the samples were sprayed with distilled water. Once the right amount of water was obtained, the pans were sealed and the tests were carried out. The water contents of the samples were 10%, 20% and 30% (w/w). All measurements were carried out under a nitrogen atmosphere (20 mL/min). Hermetic stainless steel pans were used.

Thermal gravimetric analysis (TGA) was performed in a Perkin-Elmer TGA-4000 instrument. Samples of around 10 mg were heated from 50 °C to 900 °C at a heating rate of 5 °C/min. The sample atmosphere was purged with a dry nitrogen gas flow of 20 mL/min.

2.5. Morphological characterization

The morphology of the silk specimens was assessed with a Nanosurf Easyscan 2 Atomic Force Microscope (AFM) in the dynamic mode. A cantilever with a nominal spring constant of 42 Nm^{-1}, resonance frequency of 179 kHz and a tip radius lower than 10 nm was used.

2.6. Solid state FTIR spectroscopy

Native silk samples were prepared by grinding the silk with KBr, with the help of a mortar and a pestle. A fine powder was obtained, which was used to produce pressed pellets for the FTIR spectroscopy. Regenerated spidroin films were tested directly. FTIR spectra were recorded on a Perkin-Elmer 237 spectrophotometer at room temperature (26 °C), with a nominal resolution of 4 cm^{-1} on the single-beam mode. An average of 500 scans at intervals of 1 cm^{-1} was performed on a frequency range between 4000 cm^{-1} and 400 cm^{-1}.

3. Results and discussion

Representative thermograms showing all samples tested at 10% of water content are depicted in Fig. 1. Each thermogram showed a step change associated to a thermal transition. Table 1 shows the values of such transitions for all the samples tested at different water contents.

For the sake of comparison, silkworm silk samples were also tested. The thermograms of silkworm silk are in agreement with previous DSC tests performed in the past [32,33]. The spider silk thermograms shown here are similar to the silkworm silk thermograms. All of them show a thermal transition at 170–190 °C. To the best of our knowledge, this is the first time that a DSC thermogram of spider silk shows a thermal transition that can be confirmed as repeatable and reproducible. This can be accounted for the relatively large mass used in each test (10 mg).

Table 1
Thermal transitions of silk samples.

State	Samples/water content	Thermal transition temperature (°C)			
		5%	10%	20%	30%
Native	Forced dragline silk	197	195	190	180
	Egg sac silk	171	169	164	151
	Silkworm silk fibroin	191	182	182	181
Regenerated	Dragline film	213	198	193	179
	Egg sac film	195	178	174	173

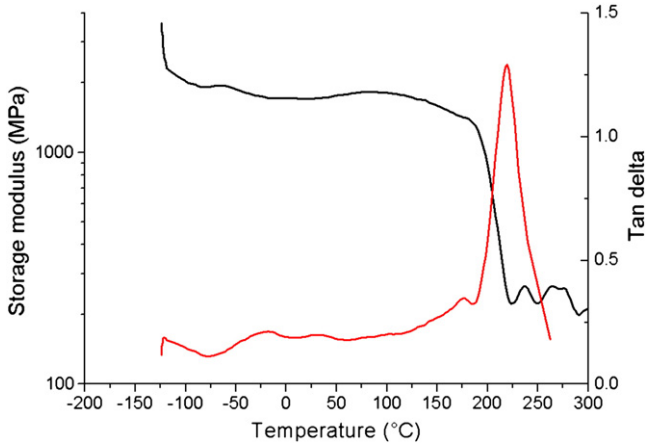

Fig. 2. Representative DMA curve showing storage modulus and tan of delta of a spider dragline silk fibre.

In the case of native egg sac silk and regenerated egg sac film, these thermal transitions have not been previously reported in the literature. The difference between the thermal transition temperature found for egg sac silk samples and dragline samples could be due to the different composition of the amino acid on each type of fibre. In fact, tubuliform and acinifom silk are used for the construction of protective egg cases and are composed by glycine, alanine and high serine content [2]. By contrast, dragline silk has a low content of serine. The hydrophilic nature of serine might enhance the plasticizing role of water, thus lowering the Tg.

Fig. 2 shows the storage (E′) and loss (E″) moduli of spider silk obtained from DMA tests in the tension mode. As can be observed in the loss modulus curve the same thermal transition observed with DSC (at around 160–200 °C) occurs at around 200 °C in the DMA tests. Other studies have reported DMA tests on dragline spider silk and found two local transitions at around −70 °C and 200 °C [24,37,38]. Vollrath et al. [37] argued that these transitions can be attributed to two different glass transition events in the disordered fraction of spider silk. The first event would be due to interactions between the hydrocarbon side chain groups while the second event would be due to the breakdown of the intermolecular hydrogen bonds in the non crystalline fraction of spider silk fibres, indicating that this fraction had started to enter the rubbery state [38].

It is reasonable to consider that the thermal transitions obtained from our DSC tests correspond to a glass transition. Several authors [37–39] have proposed that spider silk is a semicrystalline material made of amorphous and crystalline domains. The crystalline domains are believed to be formed by hydrogen bonded β-sheets while the

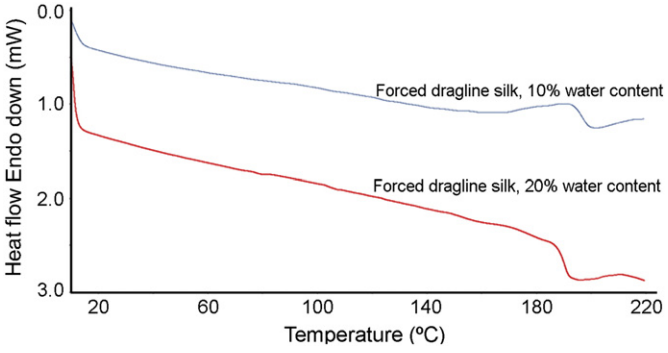

Fig. 3. Representative thermograms of native dragline silk with 10% and 20% in water content.

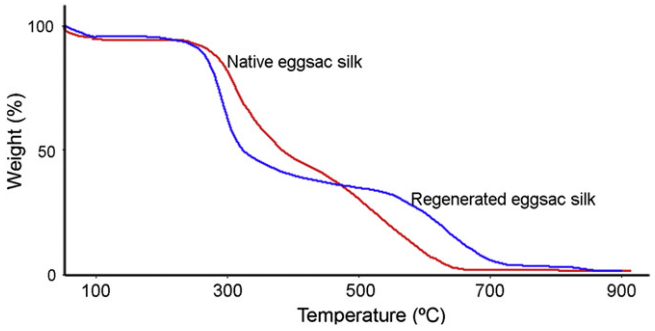

Fig. 4. Representative TGA thermograms of native spider egg sac and regenerated egg sac film.

amorphous regions are attributed to kinetically free oligopeptide chains rich in glycine.

Vollrath and others [37–39] have defined the spider silk structure in terms of order and disordered fractions of peptide segments. Ordered segments are characterized by two hydrogen bonds between amide groups, whereas disordered segments are characterized by one hydrogen bond between amide–amide interactions. Porter and Vollrath [40] have proposed that the main thermal transition observed in spider silk is similar to a polymeric glass transition. They have suggested that such glass transition is a thermal event related to a protein denaturation process and used the Lennard-Jones function for polymer group interactions to calculate a Tg for spider silk of ≈200 °C which is in good agreement with the experimental values found here.

DSC tests show that a glass transition is present on both native and regenerated dragline silk, egg sac silk and silkworm silk. Moreover, the temperature at which this glass transition takes place depends on the water content of the sample (Fig. 3). This suggests that water acts as a plasticizer and the glass transition temperature drops as the water content of the sample rises. The amorphous segments on spider and silkworm silk are held together by hydrogen bonds that are broken at the onset of the glass transition. The presence of water ncreases the molecular chain dynamics of the oligopeptide chains present in the amorphous region and, thus, the energy needed for the onset of the glass transition is lower than the value expected in the dry state [41].

The effect of water on the physical properties of spider silk has been reported in the past. It has been showed that water content has a major effect on spider silk [4]. After being immersed in water, spider silk shrinks by approximately 40–50 %, and its mechanical properties change. Its initial stiffness drops by three orders of magnitude [11]. Termonia [39] has claimed that water has a plasticizing effect on the amorphous phase of spider silk by preventing the formation of hydrogen bond between polymer chains. Elices et al. [42] have observed

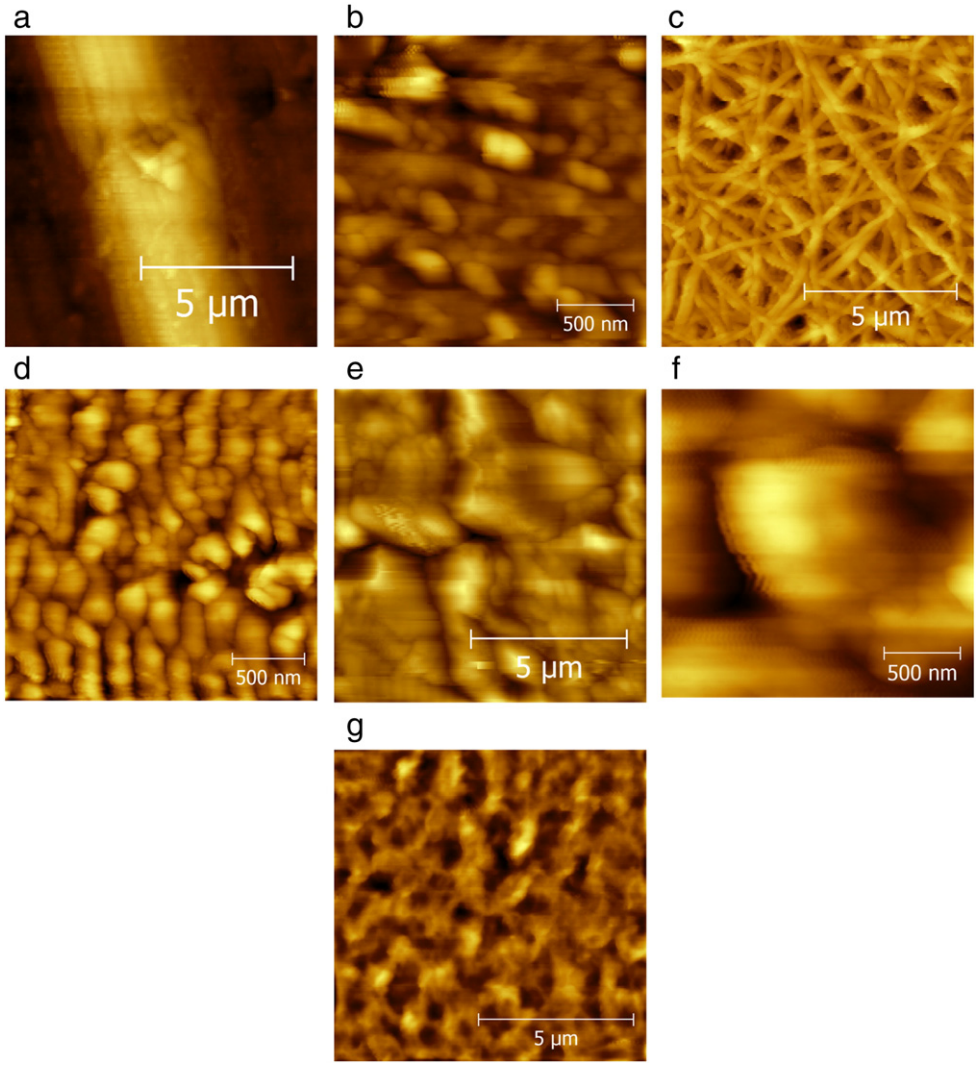

Fig. 5. AFM micrographs of native dragline silk (a) (b), native egg sac silk (c) (d), regenerated dragline film (e) (f) and regenerated egg sac film (g).

that the mechanical properties of spider silk are severely influenced by humid environments giving rise to significant decreases in its elastic modulus.

It is worth noting that a similar thermal behaviour is observed for both, native and regenerated silks. They both present a glass transition and they are affected by water content in the same way. TGA tests show also a similar behaviour with regard to water loss for both native and regenerated spider silk (Fig. 4). The weight of the sample decreases remarkably with increasing temperature above 300 °C. At 800 °C the samples were completely degraded.

The structure at the nano-level is shown in Fig. 5. Fig. 5a shows a sample of native dragline silk. The diameter of the dragline fibres studied here was around 5 μm. Fig. 5b shows the same dragline sample at a higher magnification. Globular regions of around 200 nm can be observed in this picture, which are in agreement with similar globular regions have been reported in other silk morphology studies [43,44]. Du et al. [45] have argued that these globular regions are interlinked with each other and form nano-fibrils. They have proposed that these globular regions represent the regions formed by harder materials such as protein polypeptide networks interlinked by soft (or flexible) polypeptide chains.

Fig. 5c and d show a native egg sac silk sample. The egg sac is formed by rather small fibres ranging 200–300 nm in diameter (Fig. 5c). The globular regions depicted in Fig. 5d are around 200 nm in length by they seem to be more tightly packed when compared to those observed in dragline silk. Dragline silk was obtained by using a forced silking process. It has been reported somewhere else that forced silking might alter the morphology of spider silk changing the size and arrangement of the globular regions [45].

By contrast, egg sac and dragline regenerated films (Fig. 5e, f, g, h) display a different morphology. The globular regions are not clearly depicted in these samples. This difference could be due to the fact that nano-fibrils (formed by interlinked globular regions) are not present in regenerated films, although further studies on controlled morphological characterization would be needed to confirm this.

Contamination due to the processing technique used to obtain the regenerated films could also affect the AFM images of such films. FTIR (Fig. 6) was used to determine if the ionic liquid (BMIC) used for dissolving the silk was completely removed during the methanol bath. It has been reported [46] that the aliphatic segments of BMIC show a sharp band at 2850 cm^{-1}. This band was not observed in the spectrum of regenerated films. This result is in agreement with other studies that also used methanol rinsing to remove BMIC [47,48].

Also, the FTIR tests show similar spectra for all the silk types studied (Fig. 6). The band at 1650 cm^{-1} is associated to the C═O stretching of the amide I group [49,50]. The absorption band at 1540 cm^{-1}

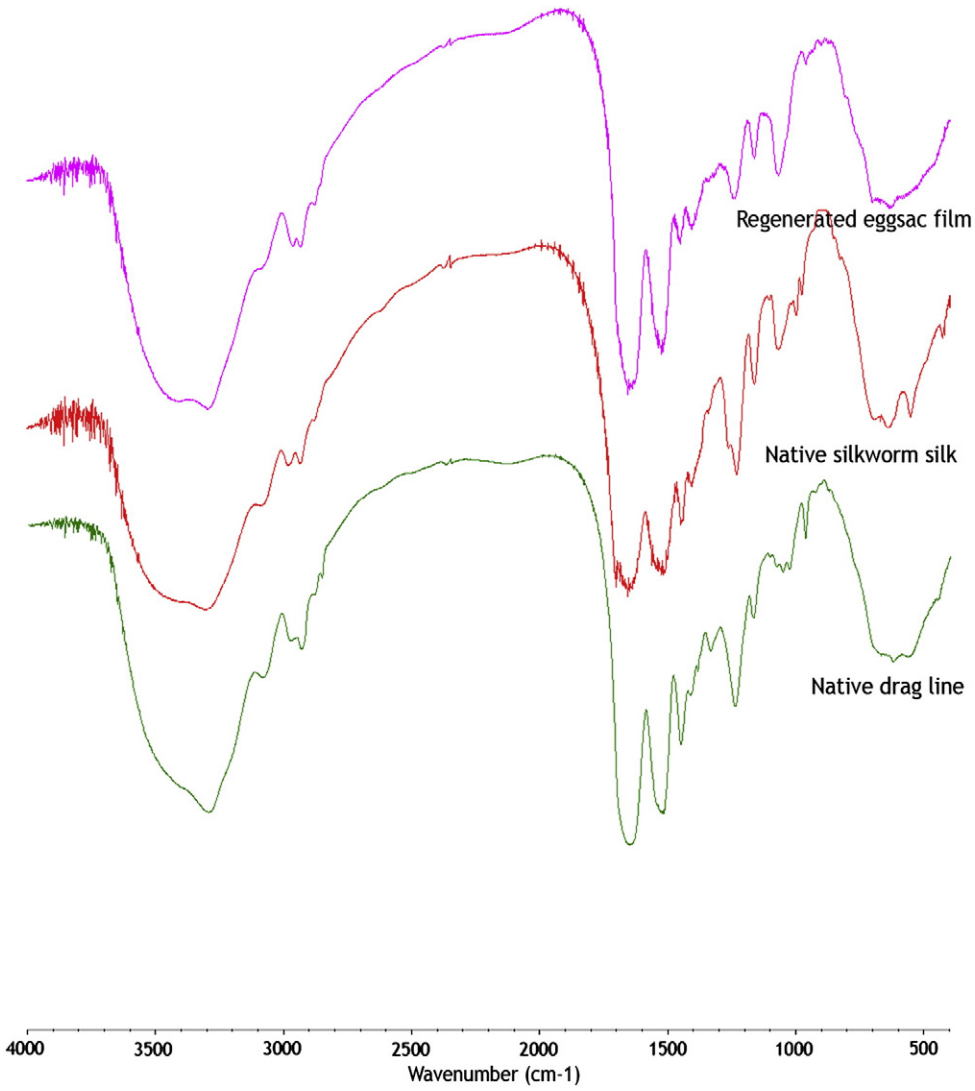

Fig. 6. FTIR spectra of native dragline silk, native silkworm silk and regenerated egg sac film.

corresponds to the N–H deformation and C–N stretching of amide II [51]. The amide III group shows three absorption bands [52] at 1384 cm^{-1}, 1339 cm^{-1} and 1238 cm^{-1}.

It is clear that the thermal transitions of the different types of silk studied here are rather similar. Conversely, the mechanical properties reported in the literature such as Young's modulus, maximum stress and maximum strain are different for each type of silk. Dragline spider silk shows a maximum stress and Young's modulus of 1.7 GPa and 30 GPa [21], whereas silkworm silk shows a maximum stress and Young's modulus of 230 MPa and 18 GPa [53]. The regenerated films obtained in our experiments show a rather brittle behaviour, with mechanical features that are too low to be measured in the way silk fibres are tested. The reason for this rather contradictory behaviour between thermal and mechanical properties for the different types of silk can be rationalized as follows. The thermal transitions observed in our experiments might be related to the amorphous regions of the materials, whereas the differences in mechanical properties between the different types of silk might be related to the size of the crystalline regions. Other factors such as crystallinity, crystalline structure and its distribution could also affect the mechanical properties of the different spider silks [54].

4. Conclusions

The thermal transitions of native and regenerated spider silk and silkworm silk have been studied and documented for the first time by means of differential scanning calorimetry. The thermal transitions for forced dragline silk, egg sac film, silkworm silk and regenerated silk films occur at around 200 °C. This value is in agreement with reported values of thermal transitions of spider silk that are associated with a glass transition. Also, water was found to act as a plasticizer in native and regenerated spider and silkworm silks as it lowers the glass transition temperature. Morphological characterization assessed by means of AFM showed similar characteristics between the different types of native silk studied. Globular regions were not observed in the regenerated specimens. FTIR showed that the regeneration process had not left traces of contaminants, confirming that all types of silk studied displayed similar spectra. The fact that we have found similar glass transitions for the different types of silks studied here, while their mechanical properties remain quite different, leads us to believe that the mechanical behaviour might be controlled mainly by the ordered or crystalline region in spider silk [54].

Acknowledgements

The authors would like to thank the Vice-Rectorship for Research of PUCP for financial support. Experimental support with the DMA tests provided by Dr. Daniel Lopez at the Institute of Polymer Science and Technology of the Spanish Council for Scientific Research (CSIC, Spain) is greatly acknowledged.

References

[1] C.L. Craig, Annu. Rev. Entomol. 42 (1997) 231–267.
[2] T.A. Blackledge, C.Y. Hayashi, J. Exp. Biol. 209 (2006) 2452–2461.
[3] F. Vollrath, D.P. Knight, Nature 410 (2001) 541–548.
[4] R.W. Work, J. Arachnol. 9 (1981) 299–308.
[5] R.W. Work, C.T. Young, J. Archnol. 15 (1987) 65–80.
[6] C.Y. Hayashi, T.A. Blackledge, R.V. Lewis, Mol. Biol. Evol. 21 (2004) 1950–1959.
[7] J. Gatesy, C. Hayashi, D. Motriuk, J. Woods, R. Lewis, Science 291 (2001) 2603–2605.
[8] M. Xu, R.V. Lewis, Proc. Natl. Acad. Sci. U. S. A. 87 (1990) 7120–7124.
[9] J. Perez-Rigueiro, G.R. Plaza, F.G. Torres, A. Hijar, C. Hayashi, G.B. Perea, M. Elices, G.V. Guinea, Int. J. Biol. Macromol. 46 (2010) 555–557.
[10] R.W. Work, N. Morosoff, Text. Res. J. 52 (1982) 349–356.
[11] J.M. Gosline, M.W. Denny, M.E. DeMont, Nature 309 (1984) 551–552.
[12] G.V. Guinea, M. Elices, J. Perez-Rigueiro, G. Plaza, Polymer 44 (2003) 5785–5788.
[13] J.D. van Beek, S. Hess, F. Vollrath, B.H. Meier, Proc. Natl. Acad. Sci. U. S. A. 99 (2002) 10266–10271.
[14] C.Y. Hayashi, N.H. Shipley, R.V. Lewis, Int. J. Biol. Macromol. 24 (1999) 271–275.
[15] A.H. Simmons, C.A. Michal, L.W. Jelinski, Science 271 (1996) 84–87.
[16] D.T. Grubb, L.W. Jelinski, Macromolecules 30 (1997) 2860–2867.
[17] F. Junghans, M. Morawietz, U. Conrad, A. Scheibel, A. Heilmann, U. Spohn, Appl. Phys. A: Mater. Sci. Process. 82 (2006) 253–260.
[18] J.A. Kluge, O. Rabotyagova, G.G. Leisk, D.L. Kaplan, Trends Biotechnol. 26 (2008) 244–251.
[19] R.D. Rogers, K.R. Seddon, Science 302 (2003) 792–793.
[20] D.M. Phillips, L.F. Drummy, R.R. Naik, H.C. de Long, D.M. Fox, P.C. Trulovec, R.A. Mantz, J. Mater. Chem. 15 (2005) 4206–4208.
[21] C.J. Dymek, D.A. Grossie, A.V. Fratini, W.W. Adams, J. Mol. Struct. 213 (1989) 25–34.
[22] D. Kaplan, S. Fossey, Polym. Adv. Technol. 5 (1994) 401–410.
[23] F. Vollrath, B. Madsen, Z. Shao, Proc. Roy. Soc. 268 (2001) 2339–2346.
[24] D. Porter, F. Vollrath, Z. Shao, Eur. Phys. J. E. 16 (2005) 199–206.
[25] F.G. Torres, M. Elices, G.R. Plaza, M.A. Arnedo, J. Perez-Rigueiro, G.V. Guinea, Biomacromolecules 10 (2009) 1904–1910.
[26] J. Perez-Rigueiro, M. Elices, J. Llorca, C. Viney, J. Appl. Polym. Sci. 82 (2001) 8845–8851.
[27] J. Perez-Rigueiro, M. Elices, G.V. Guinea, Polymer 44 (2003) 3733–3736.
[28] S. Osaki, Acta Arachnol. 37 (1989) 69–75.
[29] K.B. Guess, C. Viney, Thermochim. Acta 315 (1998) 61–66.
[30] P.M. Cunniff, A. Fossey, M.A. Auerbach, J.W. Song, D.L. Kaplan, W.W. Adams, R.K. Eby, D. Mahonney, D.L. Vezie, Polym. Adv. Technol. 5 (1994) 401–410.
[31] S.W. Watt, I.J. McEwen, C. Viney, Macromolecules 32 (1999) 8671–8673.
[32] T. Tanaka, J. Magoshi, Y. Magoshi, S. Inoue, M. Kobayashi, H. Tsuda, M.A. Becker, S. Nakamura, J. Therm. Anal. Calorim. 70 (2002) 825–832.
[33] T. Tanaka, Y. Magoshi, J. Magoshi, J. Therm. Anal. Calorim. 30 (2003) 111–115.
[34] T. Kameda, M. Tsukada, Macromol. Mater. Eng. 291 (2006) 877–882.
[35] M.A. Garrido, M. Elices, C. Viney, Perez-Rigueiro, Polymer 43 (2002) 1537–1540.
[36] R.W. Work, P.D. Emerson, J. Arachnol. 10 (1982) 1–10.
[37] F. Vollrath, D. Porter, Soft Matter 2 (2006) 377–385.
[38] Y. Yang, X. Chen, D. Porter, D. Knight, F. Vollrath, Adv. Mater. 17 (2005) 84–88.
[39] Y. Termonia, Macromolecules 27 (1994) 7378–7381.
[40] D. Porter, F. Vollrath, Soft Matter 4 (2008) 328–336.
[41] G.P. Holland, J.E. Jenkins, M.S. Creager, R.V. Lewis, J.L. Yarger, Chem. Commun. (Camb) 21 (2008) 5568–5570.
[42] G. Plaza, G.V. Guinea, J. Pérez-Rigueiro, M. Elices, J. Polym. Sci. B Polym. Phys. 44 (2006) 994–999.
[43] S. Putthanarat, S. Stribeck, S.A. Fossey, R.K. Eby, W.W. Adams, Polymer 41 (2000) 7735–7747.
[44] S.A.C. Gould, K.T. Tran, J.C. Spagna, A.M.F. Moore, J.B. Shulman, Int. J. Biol. Macromol. 24 (1999) 151–157.
[45] N. Du, X.Y. Liu, J. Narayanan, L. Li, M.L. MinLin, D. Li, Biophys. J. 91 (2006) 4528–4535.
[46] L. Yung, H. Ma, X. Wang, K. Yoon, R. Wang, B.S. Hsiao, B. Chu, J. Membr. Sci. 365 (2010) 52–58.
[47] H. Xie, S. Li, S. Zhang, Green Chem. 7 (2005) 606–608.
[48] D.M. Phillips, L.F. Drummy, R.R. Naik, H.C. De Long, D.M. Fox, P.C. Trulove, R.A. Mantz, J. Mater. Chem. 15 (2005) 4206–4208.
[49] D.M. Byler, H. Susi, Biopolymers 25 (1986) 469–487.
[50] S. Krimm, J. Bandekar, Adv. Protein Chem. 38 (1986) 181–364.
[51] J.L. Kirsch, J.L. Koenig, Appl. Spectrosc. 43 (1989) 445–451.
[52] S. Cai, B.R. Singh, Biochemistry 43 (2004) 2541–2549.
[53] J. Pérez-Rigueiro, M. Elices, J. Llorca, C. Viney, J. Appl. Polym. Sci. 82 (2001) 1928–1935.
[54] J.M. Gosline, P.A. Guerette, C.S. Ortlepp, K.N. Savage, J. Exp. Biol. 202 (1999) 3295–3303.